


Please cite the Published Version

Alruhaimi, Reem S, Kamel, Emadeldin M, Alnasser, Sulaiman M, Lamsabhi, Al Mokhtar and Mahmoud, Ayman M  (2025) 3-Hydroxy-3-Methylglutaryl Coenzyme-A Inhibitory Activity of Padina pavonia Terpenoids: An Integrated In Vitro and In Silico Exploration. Chemistry and Biodiversity. e00464 ISSN 1612-1872

DOI: <https://doi.org/10.1002/cbdv.202500464>

Publisher: Wiley

Version: Accepted Version

Downloaded from: <https://e-space.mmu.ac.uk/641898/>

Usage rights:  [Creative Commons: Attribution 4.0](https://creativecommons.org/licenses/by/4.0/)

Additional Information: This is an Author Accepted Manuscript of an article published in Chemistry and Biodiversity by Wiley.

Data Access Statement: The manuscript and supplementary material contain all data supporting the reported results.

Enquiries:

If you have questions about this document, contact openresearch@mmu.ac.uk. Please include the URL of the record in e-space. If you believe that your, or a third party's rights have been compromised through this document please see our Take Down policy (available from <https://www.mmu.ac.uk/library/using-the-library/policies-and-guidelines>)

Title:

**3-Hydroxy-3-Methylglutaryl Coenzyme-A Inhibitory Activity of *Padina pavonia*
Terpenoids: An Integrated *In Vitro* and *In Silico* Exploration**

Authors and affiliations:

Reem S. Alruhaimi¹, Emadeldin M. Kamel², Sulaiman M. Alnasser³, Al Mokhtar

Lamsabhi^{4,5}, Ayman M. Mahmoud^{6*}

¹Department of Biology, College of Science, Princess Nourah bint Abdulrahman University, Riyadh 11671, Saudi Arabia.

²Organic Chemistry Department, Faculty of Science, Beni-Suef University, Beni-Suef 62514, Egypt.

³Department of Pharmacology and Toxicology, College of Pharmacy, Qassim University, Buraydah 52571, Saudi Arabia.

⁴Departamento de Química, Módulo 13, Universidad Autónoma de Madrid, Campus de Excelencia UAM-CSIC Cantoblanco, Madrid 28049, Spain.

⁵Institute for Advanced Research in Chemical Sciences (IAdChem), Universidad Autónoma de Madrid, Madrid 28049, Spain.

⁶Department of Life Sciences, Faculty of Science and Engineering, Manchester Metropolitan University, Manchester M1 5GD, UK.

*Corresponding author:

Ayman M. Mahmoud

Department of Life Sciences, Faculty of Science and Engineering, Manchester Metropolitan University, Manchester M1 5GD, UK

ORCID ID: 0000-0003-0279-6500

E-mail: a.mahmoud@mmu.ac.uk

Abstract

The inhibition of 3-hydroxy-3-methylglutaryl coenzyme-A (HMGCR) activity carries considerable therapeutic significance, prompting the investigation of novel inhibitors to tackle associated health conditions and improve patient care. Seeking non statin scaffolds, we provide the first integrated evaluation of six terpenoids isolated from the brown alga *Padina pavonia*, expanding the species' chemical repertoire and establishing their activity against HMGCR. We have previously shown the anti-hyperlipidemia activity of *P. pavonia* terpenoid-rich fraction. Herein, we evaluated the inhibitory potential of six *P. pavonia* terpenoids against HMGCR, employing both *in vitro* and *in silico* methodologies. All terpenes inhibited HMGCR, with compound **1** being the most potent ($IC_{50} = 17.93 \pm 1.78 \mu M$), followed by compound **5** ($IC_{50} = 22.47 \pm 1.59 \mu M$) and compound **2** ($IC_{50} = 24.51 \pm 2.13 \mu M$). Molecular docking revealed that all compounds have affinity towards HMGCR and compounds **1** and **2** are effectively bound to the same active site as the reference drug atorvastatin. Molecular dynamics (MD) simulations depicted notable energy stabilization and consistent trajectory profiles of the terpenes-HMGCR complexes. The results of MM/PBSA analysis depicted the lowest binding free energies for compounds **1** and **5** (-7.00 ± 1.00 and -7.06 ± 2.24 kJ/mol, respectively). These findings along with the limited number of detected hydrogen bonds and the results of interaction energy calculations suggest that the formed complexes are mainly influenced by attractive forces associated with van der Waals interactions rather than electrostatic interactions. *In vitro* experiments revealed the inhibitory activity of all isolated terpenes with compound **1** exhibiting the most potent activity. Therefore, terpenoids of *P. pavonia* represent promising candidates for the development of HMGCR inhibitors.

Keywords

49 HMG-CoA reductase; *Padina pavonia*; Molecular dynamics; Terpenoids;
50 Hypercholesterolemia.

51 **1. Introduction**

52 3-hydroxy-3-methylglutaryl-coenzyme A reductase (HMGCR) is a crucial enzyme in the
53 mevalonate pathway which plays a vital role in the biosynthesis of cholesterol ^[1]. This enzyme
54 facilitates the conversion of HMG-CoA to mevalonate, a precursor for cholesterol and other
55 important compounds like dolichols, ubiquinones, and isoprenylated proteins ^[2]. Because of
56 its pivotal role in cholesterol regulation and the control of cellular processes dependent on
57 isoprenoids, HMGCR is an attractive target for developing therapeutics to manage
58 dyslipidemia and prevent cardiovascular diseases ^[3]. Dysregulated cholesterol metabolism is
59 effectively associated with the pathogenesis of cardiovascular conditions, including
60 atherosclerosis and coronary artery disease ^[4]. Thus, pharmacological inhibition of HMGCR
61 represents a cornerstone in the treatment of hypercholesterolemia and related cardiovascular
62 disorders ^[5]. Statins, which are synthetic inhibitors of HMGCR, are widely prescribed for their
63 cholesterol-lowering effects and cardiovascular benefits ^[6]. However, their use may be limited
64 by adverse effects and tolerability issues, prompting the search for alternative therapeutic
65 agents with improved safety profiles ^[6].

66 *Padina pavonia* L. (*P. pavonia*), a brown macroalga commonly found in tropical and
67 subtropical coastal regions, has gained significant interest in recent years due to its rich
68 repertoire of bioactive natural products ^[7]. With its widespread distribution and adaptability to
69 diverse marine environments, *P. pavonia* serves as a prolific source of secondary metabolites
70 with diverse chemical structures and pharmacological activities ^[8]. These bioactive
71 compounds, synthesized by the alga as part of its defense mechanism against environmental

stressors, have demonstrated promising potential for various biomedical and biotechnological applications ^[7]. The chemical constituent of *P. pavonia* included volatile oils, terpenes, fatty acids, aromatic esters, polyphenols, and sulfated polysaccharides ^[7, 9]. Given its diverse array of natural products, *P. pavonia* displayed broad spectrum pharmacological properties such as anti-inflammatory, antioxidant, hepatoprotective, anti-coagulant, antimicrobial, and antitumor activities ^[8b, 8c, 10].

Combining *in vitro* studies and *in silico* techniques, such as molecular dynamics (MD) simulations and docking analyses, provides valuable insights for investigating the inhibitory activity of natural products against enzymes ^[11]. *In vitro* studies provide valuable experimental data on the biochemical interactions between natural compounds and enzymes, offering insights into their inhibitory potency and mechanism of action ^[11a]. In parallel, *in silico studies* allow for the exploration of the molecular interactions between drugs and enzymes at the atomic level ^[12]. Docking studies predict the binding modes and affinity of natural compounds within the active site of enzymes, providing structural insights into their inhibitory mechanisms ^[13]. Additionally, MD simulations offer a dynamic perspective by simulating the behavior of drug-enzyme complexes over time, elucidating the stability and conformational dynamics of these interactions ^[14]. Integrating both *in vitro* and *in silico* approaches can enhance our knowledge of the inhibitory efficacy of terpenes against HMGCR, facilitating the rational design and optimization of novel terpene-based inhibitors for therapeutic applications ^[15].

Natural products, including terpenoids, have gained attention for their potential as HMGCR inhibitors ^[16]. These compounds offer diverse chemical structures and pharmacological properties, making them promising candidates for drug discovery and development. In our earlier findings, we documented the anti-dyslipidemic, anti-hyperglycemic, antioxidant, and

anti-inflammatory attributes of a terpenoid-enriched fraction of *P. pavonia* in a rat model of type 2 diabetes^[7]. In this study, we evaluated, for the first time, the inhibitory activity of natural terpenes isolated from *P. pavonia* against HMGCR using an integrated *in vitro* and *in silico* approach. By exploring the inhibitory potential of these compounds, we aim to identify novel lead compounds for the development of therapeutics targeting dyslipidemia and cardiovascular diseases. Through our investigation, we seek to contribute to the growing body of knowledge on natural product-based interventions for managing cholesterol metabolism and associated cardiovascular risk factors.

2. Materials and Methods

2.1. Collection of *P. pavonia*, extraction, and isolation

2.1.1. General

The Nuclear Magnetic Resonance (NMR) spectra of *P. pavonia* isolated compounds (¹H NMR and ¹³C NMR) were measured using Varian Unity Inova spectrometer. TMS was employed as the internal standard. The chemical shift values were denoted in δ (ppm), while the coupling constants were indicated as J in Hz. The UV-Vis spectra were measured using Shimadzu UV-vis 160i spectrophotometer. The optical rotation of isolated terpenes was assessed by means of Perkin-Elmer 341 polarimeter. HREIMS and EIMS analyses were recorded by means of Finnigan MAT TSQ 700 mass spectrometer. Shimadzu FTIR-8400 spectrophotometer was utilized for calculating the FTIR spectra by means of KBr pellets.

2.1.2. Alga collection and isolation of terpenes

P. pavonia chemical constituents (Fig. 1) utilized in this study were obtained from our prior investigation ^[7]. The experimental details of isolating six terpenes from *P. pavonia* are represented in our previously reported work ^[7]. In summary, *P. pavonia* was obtained from the Red Sea shoreline in Kiyal Valley and Ras Al Sheikh Humaid, Kingdom of Saudi Arabia. Subsequently, the samples underwent washing, drying, grinding, and exhaustive extraction with dichloromethane (DCM). The solvent was evaporated *in vacuo* to yield a brownish residue (32 g). The DCM extract was then suspended in water and sequentially partitioned with ethyl acetate and n-butanol, resulting in ethyl acetate and n-butanol fractions weighing 13 and 9 g, respectively. The ethyl acetate fraction was chromatographed over a silica gel column eluted with the solvent system n-hexane/ethyl acetate mixture (0-10:10-0). This process yielded 38 fractions, which were monitored by TLC and combined into 17 fractions (E1-E17) based on their TLC profiles. Subsequently, fraction E6 underwent re-chromatographing over a silica gel column, eluted with CHCl₃-methanol of increasing polarity (10:1→ 5:1), to generate seven fractions (E6.1-E6.7). Sub-fraction E6.3 was further chromatographed using ODS column chromatography (1 x 20 cm) with methanol as the eluent, affording the pure form of compound **3** (16 mg). Fraction E10 underwent silica gel column chromatography using a gradient elution of n-hexane-ethyl acetate (5:1→ 1:1), resulting in the isolation of 9 sub-fractions (E10.1-E10.9). E10.3 was subsequently purified using silica gel column (1 x 15 cm) using the solvent system n-hexane-EtOAc (2:1) as the eluent, yielding compound **4** (13 mg). Subsequently, E10.8 was purified using silica gel column with the solvent system of n-hexane-chloroform-methanol (7:5:1) as the eluent, producing 5 sub-fractions (E10.8.1-E10.8.5). Purification of sub-fraction E10.8.3 was achieved through ODS column chromatography using methanol-

water (2:1) as the eluent, resulting in the isolation of purified compound **6** (11 mg). Fraction E12 was subjected to silica gel column chromatography, eluted with n-hexane-ethyl acetate (5:1→ 1:5), generating 5 fractions (E12.1-E12.5). Then, E12.2 was further chromatographed over a Sephadex LH-20 column and eluted with acetone to yield the pure form of **1** (18 mg). Additionally, E12.5 was applied to the top of a silica gel column and eluted with a petroleum ether/acetone system (5:1→ 1:5), resulting in 5 sub-fractions (E12.5.1-E12.5.5). Compound **5** (15 mg) was obtained from sub-fraction E12.5.3 after purification over an RP-18 gel column chromatography using methanol-water (9.5:0.5) as an eluent. Sub-fraction E12.5.4 was further purified over an ODS column with methanol-water (2:1) as the eluent to yield compound **2**.

2.2. Molecular docking

The three-dimensional crystal structure of human HMGCR was retrieved from the Protein Data Bank (accession code 1DQA, Resolution: 2.00 Å, and R-Value: 0.168, chain A). *In silico* molecular docking analysis of the isolated compounds and atorvastatin (ATOR) with HMGCR was performed by means of the open-source using Tools (ADT) v1.5.6 and AutoDock Vina software packages ^[17]. Prior to docking runs, the HMGCR system underwent a series of preparation steps. These steps included the elimination of nonstandard residues and solvent molecules, the inclusion of polar hydrogens, and the adjustment of the grid box to include the significant key residues within the active site ^[13b]. These optimizations were executed using ADT v1.5.6. Binding interactions were visualized, and images were generated using PyMOL v2.4. Density functional theory (DFT) calculations were carried out using the Gaussian 16 software package ^[18]. The geometries of the isolated terpenes from *P. pavonia* (compounds 1-6) were fully optimized without constraints at the B3LYP exchange-correlation functional level ^[19], utilizing the 6-311G (d, p) basis set ^[20]. Additionally, frequency calculations were

implemented to verify that there were no imaginary frequencies present in the ground states. The D3 formalism was utilized to calculate the dispersion correction in all computations^[21], encompassing geometry optimizations, frequency analyses, and single-point energy determinations, to guarantee precise dispersion-corrected energies^[22].

2.3. Molecular dynamics simulations

The complexes of *P. pavonia* isolated terpenoids with HMGCR (PDB ID: 1DQA), exhibiting the minimum binding affinities as calculated by docking runs, were selected for further MD simulations. The topology and geometric characteristics of the terpenoids were created using the CGenFF tool (<https://cgenff.umaryland.edu/>). The obtained parameters were then incorporated into the topology of HMGCR. The open-source GROMACS 2022.4 software was used for performing the MD simulations calculations^[23], using the all-atom CHARMM36 force field^[24]. The free target enzyme and different terpenoid systems were placed within a dodecahedron box with periodic boundary conditions, resulting in a box volume of 859.63 nm³. The CHARMM-modified TIP3P water model was utilized, and electrical neutrality was maintained by adding one chloride counter-ion^[25]. The thermodynamically unfavorable interactions was mitigated by performing 10 ps steepest descent energy minimization process^[26]. Energy minimization was performed using the steepest descent algorithm until a maximum force below 1000.0 kJ/mol/nm was achieved. This was followed by a two-stage equilibration process. The first stage involved the NVT ensemble (constant number of particles, volume, and temperature) for 100 ps at 300 K using the V-rescale thermostat with a coupling constant of 0.1 ps. The second stage involved the NPT ensemble (constant number of particles, pressure, and temperature) for 100 ps at 300 K and 1 bar using the Parinello-Rahman barostat with a coupling constant of 2.0 ps^[27]. Finally, 30 ns MD simulations were executed at a temperature

of 300 K and a pressure of 1 bar. The leap-frog integrator was used with a time step of 2 fs. The LINCS algorithm was employed to constrain all bond lengths, and long-range electrostatics were handled using the Particle Mesh Ewald (PME) method with a cutoff of 1.2 nm for both Coulomb and van der Waals interactions. Trajectories were saved every 10 ps for subsequent analysis.

The binding free energies of the tested terpenes against HMGCR were calculated using the Molecular Mechanics/Poisson-Boltzmann Surface Area (MM/PBSA) method ^[28]. The gmx_MMPBSA tool was employed for this purpose ^[29]. This tool integrates molecular mechanics, Poisson-Boltzmann electrostatics, and solvent accessibility models to estimate the binding energies. The calculations were performed based on the obtained MD simulation trajectories to obtain detailed insights into the interactions between the compounds and the enzyme.

2.4. HMGCR inhibitory activity assay

The *in vitro* inhibition assay of investigated compounds on HMGCR was performed as previously described ^[30]. In a 96-well plate, 20 µl of different concentrations (0-100 µM) of various drugs under investigation were mixed with 40 µl HMGCR (4 U/mL), 80 µl HMG-CoA and 20 µl 0.1 M phosphate buffer (pH 7.0) and the mixture was incubated for 5 min at 37 °C. Forty µl of 100 µM NADPH was added and the absorbance was read at 340 nm following incubation for 15 min at 37 °C. Phosphate buffer instead of the enzyme and test compounds was used in the blank and control, respectively, and the experiment was carried out three times independently. The inhibition kinetics of were analyzed using different concentrations of the test compound and substrate and the Lineweaver–Burk plot was constructed using GraphPad Prism 8.0 software (San Diego, CA, USA).

3. Results and discussion

3.1. Isolated chemical constituents

The ethyl acetate-soluble fraction from *P. pavonia* underwent a sequential of chromatographic investigation steps using various stationary phases. This process resulted in the isolation of six terpenes which had not been previously reported in this species. The chemical structures of the isolated terpenes were determined through spectroscopic analyses (Suppl. material) and data comparison with previously reported information ^[7]. Consequently, the isolated compounds (Fig. 1) were identified as 3 α -hydroxy-5,6-epoxy-7-megastigmen-9-one (**1**) ^[31], oplodiol (**2**) ^[32], loliolide (**3**) ^[33], (6R,7E,9R)-9-hydroxy-4,7-megastigmadien-3-one (**4**) ^[34], petasol (**5**) ^[35], and (+)-dehydrovomifoliol (**6**) ^[36].

3.2. Molecular docking

A molecular docking simulation was employed to investigate the binding modes of terpenes from *P. pavonia* with HMGCR. As shown in Table 1, the isolated terpenoids exhibited promising binding affinities, indicating strong interactions with the target enzyme. The observed binding energies of the isolated terpenes indicate their potential inhibitory activity against HMGCR. However, the activities of individual compounds are not largely discriminated because of the comparable binding affinities obtained, ranging from -5.5 to -6.0 kcal/mol. After several attempts that accounted for binding affinities and the position of ligands within the HMGCR binding pocket, we chose the thermodynamically favored docking pose for each terpene-HMGCR system. Figures 2 and 3 represent the results of the docking assessments, portraying how various terpenoids are spatially arranged within the active site of HMGCR. These figures also emphasize the amino acid residues involved in both polar and hydrophobic interactions with the examined compounds. Importantly, compounds **1** and **2**

effectively docked into the same binding site as the positive control ATOR, indicating their potential to inhibit enzyme activity. Conversely, compounds **3-6** occupied a different binding pocket other than that of compounds **1** and **2**. The highest extent of polar interaction was detected in compounds **4** and **6** complexes, whereas the remaining compounds displayed only one polar bond with the target enzyme. On the other hand, a large number of hydrophobic interactions was detected in the binding mode of all investigated drugs against HMGCR. Moreover, the hydrophobic binding profiles of compounds **3** and **5** indicated the involvement of a single phenylalanine residue (Phe628), recognized for its contribution to thermodynamically favorable π - π interactions. These findings underscore the varied modes of interaction between isolated terpenes and HMGCR, implying potential diversity in their mechanisms of inhibiting the target enzyme. Moreover, the participation of crucial key residues in the binding profiles of these compounds implies their potential inhibitory mechanisms against HMGCR. Hence, the results of the docking analyses indicated a notable preference for the inhibitory potential of compounds **1** and **2** against the target enzyme. Subsequent investigation of these interactions could contribute to the formulation of novel therapeutic agents targeting HMGCR, potentially offering remedies for various medical conditions.

3.3. MD simulations

In this investigation, we presented the results of our MD simulations which aimed to elucidate the dynamic behaviors and stabilities of complexes formed between HMGCR and isolated terpenes. MD simulations are a powerful tool for examining the temporal evolution and structural dynamics of drug-enzyme interactions at the atomic scale ^[11b]. Through these simulations, we gained comprehensive insights into the stabilities, flexibilities, and conformational changes exhibited by complexes comprising terpenoids from *P. pavonia* and

252 HMGCR, under simulated environmental conditions over time. The objective of these
253 simulations is to elucidate the molecular mechanisms governing the catalytic
254 biotransformation of *P. pavonia*-isolated terpenes within the binding site of HMGCR. To figure
255 out the concordance between tested drugs and the binding site of HMGCR, we conducted MD
256 simulations using the GROMACS package over a 30 ns timeframe. Specifically, we focused
257 on complexes with the minimum binding affinity identified from docking analysis for each
258 compound. Subsequently, we conducted an in-depth analysis of the MD trajectories with
259 particular focus on important MD parameters including interaction energies, hydrogen bonding
260 profiles, root mean square deviations (RMSD), radius of gyration (Rg), root mean square
261 fluctuations (RMSF), and solvent accessible surface area (SASA). This comprehensive
262 analysis encompassed both free enzyme and various isolated terpenes-HMGCR complexes.

263 The CHARMM36 all-atom forcefield was selected for its robust performance in accurately
264 modeling protein-ligand interactions and its compatibility with a wide range of biomolecular
265 systems ^[24]. We employed the CHARMM-modified TIP3P water model, which is known for
266 its effectiveness in simulating the structural and thermodynamic properties of biological
267 molecules in aqueous environments, including proteins and nucleic acids ^[37]. This combination
268 ensures reliable and realistic simulation outcomes, which are crucial for interpreting the
269 interactions between HMG-CoA reductase and *P. pavonia* terpenoids.

270 3.3.1. Structural stability and dynamics properties

271 The assessment of RMSD provides vital insights into the structural stability and
272 conformational changes of biological macromolecules during MD simulations ^[11b]. In our
273 analysis, we specifically examined the deviation of atomic positions, with a focus on backbone
274 RMSD values, across different systems relative to the free HMGCR, which act as the reference

structure during the simulation period. As shown in Figure 4A, it is apparent that during the first five ns of the initial equilibration, both the free HMGR and the different complexes showed a rising trend in their backbone RMSD values. Subsequently, these RMSD profiles stabilized and fluctuated to the end of the duration of the simulation. The observed high fluctuation profile of the RMSD values for the isolated terpenes-HMGCR complexes indicates that these complexes undergo significant structural changes over time during the MD simulation. Except for compound **4**, all tested complexes exhibited higher RMSD values compared to the free enzyme, suggesting that these drug molecules may induce more pronounced deviations from the enzyme original conformation. This could imply that these drugs interact with the enzyme in a manner that disrupts its stability or induces conformational changes, potentially affecting its function or activity. Remarkably, compounds **1** and **5** exhibited notably high RMSD values post-equilibration, indicating substantial structural changes or flexibility within the enzyme-drug complex. These variations are because of the dynamic interactions between these compounds and the binding site of HMGCR, potentially reflecting its ability to adjust its binding conformation for effective inhibition. Conversely, compound **4** displayed the lowest RMSD values, suggesting structural stability and robust binding within the enzyme active site. These low RMSD values imply a steady conformation with minimal structural fluctuations during enzyme interaction, facilitating potent inhibition of HMGCR activity. However, RMSD fluctuations observed for all tested drugs fall within the range for stable complexes, indicating relatively stable binding configurations with the enzyme throughout the simulation.

In order to figure out the structural variations of terpenes molecules distinct from their interaction with HMGCR, we calculated the RMSD values of studied terpenes (Fig. 4B). This

involved aligning the trajectory frames to the primary drug conformation followed by estimating the RMSD of the drug coordinates relative to this reference. The proposed methodology allows us to assess the deviation of the inhibitor from its initial geometry. Such an approach is pivotal in drug design inquiries focused on estimating the stability and dynamic behavior of proposed drugs. As shown in Figure 4B, the study of RMSD for various terpenes showed a significant variation in their RMSD patterns. The elevated fluctuation behavior observed in the drug-to-drug RMSD values for compound **1** compared to other drugs may suggest a higher degree of structural variability or dynamic flexibility within the compound . The heightened fluctuation could point out that compound **1** undergoes more pronounced conformational changes or exhibits greater adaptability in its binding conformation with the target enzyme. Such behavior might influence its interactions with HMGCR and significantly impact its inhibitory efficacy or binding stability. The observation that all tested drugs exhibited a perfectly equilibrated drug-to-drug RMSD profile suggests that these compounds maintain consistent structural stability and conformational behavior throughout the simulation period. This equilibrium indicates that the drugs undergo minimal fluctuation or deviation from their initial conformations while interacting with the target enzyme. Such stability in RMSD profiles implies that the drugs maintain relatively constant binding configurations and interactions with the enzyme, which could contribute to their inhibitory activity and effectiveness in binding to the target site.

Next, we investigated the binding characteristics of the investigated drugs in the binding pocket of HMGCR by assessing the hydrogen bonding profiles of different terpenes-HMGCR systems during the 30 ns simulation period, as illustrated in Figure 5A. The examination of hydrogen bonds revealed the presence of only two strong hydrogen bonding for all tested drugs. The

occurrence of only two hydrogen bonds in the hydrogen bonding profile resulting from MD calculations suggests that the interactions between the drug and the enzyme may be primarily driven by other forces, such as hydrophobic interactions or van der Waals forces. This limited number of hydrogen bonds could indicate a specific binding mode where only a few key interactions are involved in stabilizing the drug-enzyme complex. Additionally, it may imply a more selective or constrained binding orientation in the binding site of the HMGCR, where only certain functional groups of the drug are involved in forming hydrogen bonds with oxo moieties of HMGCR. Then, we evaluated the time-averaged RMSF profile for the free HMGCR and various terpenes complexes, with the objective of assessing the local mobility of the protein, as illustrated in Figure 5B. This graph depicts RMSF values plotted against residue numbers over a 30 ns trajectory. As expected, the RMSF values of HMGCR-terpenoids complexes exhibited patterns akin to that of the free HMGCR, suggesting negligible variations in the mobility or flexibility of the target enzyme active residues. Consequently, it can be inferred that the tested drugs displayed no effect on the conformational of the target enzyme.

The exploration of dynamics and stability across various complexes was aided by analyzing Rg values^[38], which act as measures of enzyme compactness, reflecting changes in folding, unfolding, and conformational transitions during simulation^[38]. The Rg values for both the unbound HMGCR and different flavonoid complexes were computed and are depicted in Figure 6A. The observed fluctuation pattern in the Rg values among the tested drug-HMGCR complexes suggests variability in their structural compactness and conformational stability over the simulation period. Specifically, the complex involving compound **1** exhibited the lowest Rg values following equilibration and throughout the latter half of the simulation. This indicates a high compactness and minimum energy conformation of the compound **1**-HMGCR

complex compared to other complexes, suggesting potentially stronger binding interactions or a more favorable binding orientation within the enzyme's active site. Similarly, compound **2** displayed low Rg values, suggesting its activity against the target enzyme. Additionally, it's noteworthy that the free enzyme also exhibited high fluctuation in its Rg values. This could indicate inherent flexibility or conformational dynamics of the enzyme in the absence of ligand binding, which is consistent with the behavior of enzymes in solution. SASA is commonly utilized to gauge the interaction dynamics between enzymes and solvents, providing crucial insights into conformational variations throughout the binding interactions and assessing enzyme accessibility ^[11b]. The fluctuations in SASA through studied complexes are illustrated in Figure 6B. The similarity in SASA values between all tested drugs and the unbound enzyme suggests minimal alteration in enzyme accessibility upon drug binding. Similarly, akin to the Rg profile, compound **1** exhibited the lowest SASA value, indicating potential stabilization within the enzyme active site.

The interaction between *P. pavonia* terpenoids and HMG-CoA reductase was analyzed by examining changes in the SASA upon ligand binding. The results indicate a significant reduction in SASA for the enzyme-terpenoid complexes compared to the free enzyme, suggesting that the binding of terpenoids induces conformational changes that decrease solvent exposure. This reduction in SASA reflects the stabilization of the protein-ligand complex through close contact interactions. Furthermore, the initial binding of a terpenoid appears to facilitate subsequent binding events by altering the SASA of adjacent binding sites, demonstrating a positive cooperative effect. These observations suggest that the binding of one terpenoid enhances the accessibility and affinity of other terpenoid molecules, thereby promoting cooperative binding behavior. This cooperativity is crucial for the inhibitory

potency of the terpenoids, as it leads to more efficient enzyme inhibition through the stabilization of multiple ligand-binding events.

3.3.2. Interaction energy calculations

The assessment of interaction energies including short-range Coulombic(Coul-SR) and Lennard-Jones(LJ-SR) of drug-enzyme systems yields crucial insights into the electrostatic and van der Waals interactions between the drug molecule and the enzyme. Coul-SR interactions denote the electrostatic forces between charged particles, while LJ-SR interactions encompass van der Waals interactions ^[39]. Studying these interactions offers insight into the precise interaction mechanisms between the drug and target enzyme binding cavity, provides information on the kinetics of complex formation, and contributes to figuring out the molecular mechanisms governing drug-receptor interactions. Illustrated in Figure 7 are the interaction energies HMGCR and the tested terpenoids, with a focus on Coul-SR and LJ-SR interactions. The results of calculating average Coul-SR and LJ-SR energies for different terpenoids-HMGCR complexes are shown in Table 2. Figure 7A represents the Coul-SR energy profile of different tested terpenoids-HMGCR systems. This energy profile reached equilibrium at the beginning of the simulation then fluctuated normally for the rest of the simulation time. Compound **5** exhibited the lowest average Coul-SR interaction energy (-50.89 ± 2.2 kJ/mol), indicating strong electrostatic interactions with HMGCR binding pocket. These interactions likely entail advantageous charge-charge interactions between the terpene and particular enzyme residues, enhancing its inhibitory effectiveness. The range of average Coul-SR interaction energies observed across all tested drug complexes spans from approximately -2 to -50 kJ/mol. This variation suggests differing strengths of electrostatic interactions between various drugs and the active site of HMGCR, potentially influencing their inhibitory potency.

390 The average Coul-SR-RMSD values, ranged from approximately 9 to 17 nm. This wide range
391 indicates considerable fluctuations in the position of the drug molecules within the active site
392 of HMGCR throughout the simulation period. These fluctuations may reflect dynamic
393 interactions between the drugs and the enzyme, potentially affecting their binding affinity and
394 inhibitory activity. In contrast, the LJ-SR interaction energies depicted in Figure 7B served as
395 reliable indicators for assessing binding interactions. It is noteworthy that all tested drugs
396 achieved early equilibration at the beginning of the simulation time, except for compounds **1**
397 and **3**, which reached equilibrium after approximately 7.5 ns. The observation that compounds
398 **1** and **3** complexes exhibited less negative LJ-SR interaction energies compared to other
399 compounds suggests that these particular complexes may engage in stronger van der Waals
400 interactions within the binding site of the enzyme. Conversely, the LJ-SR interaction energy
401 values observed for other compounds imply that they may interact with the enzyme through
402 similar van der Waals forces, albeit with varying degrees of strength. The inhibitory activity of
403 tested drugs stems from its engagement in attractive forces with complementary residues in the
404 enzyme, particularly through non-polar regions. The isolated terpenes likely adopt a binding
405 pose or conformation that optimizes favorable van der Waals interactions with the enzyme.
406 This observation aligns with the findings of docking analysis, underscoring the significance of
407 hydrophobic interactions in the binding mechanism of isolated compounds to HMGCR. The
408 lower average LJ-SR interaction energies detected across all tested systems (ranging from \approx -
409 18 to -84 kJ/mol) suggest a predominant contribution of van der Waals interactions compared
410 to electrostatic interactions. This indicates that the binding stability of the complexes is
411 primarily driven by attractive forces associated with van der Waals interactions rather than
412 Coulombic interactions. This observation suggests that hydrophobic binding mechanism, such

as dispersion forces, predominantly contribute to stabilizing tested complexes. Moreover, the characteristic fluctuations and more negative values of both Coul-SR and LJ-SR energies indicate energy minimized interactions between some tested drugs and the target enzyme. Consequently, these complexes exhibit a balanced combination of kinetic and energetic favorability, with a dominant interaction type. Additionally, minor structural modifications and fluctuations around the energetically favorable state are anticipated in different systems, suggesting a steady and dynamically equilibrated binding configuration.

3.3.3. MM/PBSA analysis

The MM/PBSA calculations were performed to estimate the binding free energies of six tested terpenes against HMGCR. The results are summarized in Table 3, detailing the van der Waals energy (ΔE_{vdw}), electrostatic energy (ΔE_{ele}), solvation free energy (ΔG_{solv}), gas phase energy (ΔG_{gas}), and the total binding free energy (ΔG_{total}). Compound **1** exhibited a significant van der Waals interaction energy and electrostatic interaction energy. The solvation energy was positive, indicating an unfavorable solvation contribution. The total binding free energy for compound **1** was -7.00 ± 1.00 kcal/mol, suggesting a strong binding affinity to HMGCR. Similar to compound **1**, compound **2** also demonstrated significant van der Waals and electrostatic contributions. The solvation free energy was slightly lower, resulting in a comparable total binding free energy, indicating a strong binding interaction. Compound **3** showed weaker van der Waals and electrostatic energies. This indicates a relatively weaker interaction with HMGCR. Compound **4** had the least favorable van der Waals and electrostatic interactions. The positive solvation energy further contributed to a total binding free energy of 0.32 ± 0.55 kcal/mol, indicating that Compound **4** is unlikely to effectively bind to HMGCR. Compound **5** exhibited van der Waals and electrostatic energies similar to compounds **1** and **2**.

However, it had a higher solvation energy, leading to a total binding free energy ($\Delta G_{\text{total}} = -7.06 \pm 2.24$ kcal/mol), suggesting a strong binding affinity. Compound **6** displayed moderate van der Waals and electrostatic interactions, indicating a moderate binding affinity. Overall, these findings suggest that compounds **1**, **2**, and **5** are promising candidates for further development as inhibitors of HMGCR. The relatively high binding affinities indicate their potential efficacy in modulating the enzyme's activity, which could be beneficial for therapeutic applications targeting cholesterol biosynthesis pathways.

3.4. *In vitro* HMGCR inhibition

The inhibitory activity of the isolated compounds and atorvastatin on HMGCR was evaluated *in vitro* (Fig. 8). All compounds showed HMGCR inhibitory activity with compound **1** exhibited the most potent activity and the lowest IC_{50} value (17.93 ± 1.78 μ M, Fig. 8A), followed by compounds **5** (22.47 ± 1.59 μ M, Fig. 8E), **2** (24.51 ± 2.13 μ M, Fig. 8B), **6** (26.53 ± 1.68 μ M, Fig. 8F), **3** (39.97 ± 1.98 μ M, Fig. 8C), and **4** (65.17 ± 2.41 μ M, Fig. 8D). Given its highest inhibitory activity against HMGCR, we investigated the enzyme kinetics of compound **1** as depicted in Figure 9A-B. Michaelis–Menten plots revealed a clear, concentration-dependent decrease in reaction velocity even at low micromolar inhibitor levels (Fig. 9A). Analysis of the inhibitory activity of compound **1** using Lineweaver–Burk analysis curve revealed a mixed inhibition mechanism (Fig. 9B) with inhibition constant (K_i) value 2.95 μ M. Thus, these results reveal that compound **1** can bind to both the free enzyme and the enzyme–substrate complex, demonstrating its efficacy as an HMGCR inhibitor for employment in therapeutic purposes.

Compared with prior natural HMGCR inhibitors, the *P. pavonia* terpenes fall in the low-to-mid micromolar range and are thus within the more active band for non-statin scaffolds. Our lead

compound **1** shows IC_{50} of $17.93 \pm 1.78 \mu M$ and $K_i = 2.95 \mu M$ (mixed-type), with the series spanning 22.47–65.17 μM across compounds **5**, **2**, **6**, **3**, and **4**. Potent small natural molecules reported previously include curcumin ($IC_{50} = 4.3 \mu M$) and salvianolic acid C (8 μM) against human HMGCR, highlighting that single-digit micromolar potency is achievable for non-statins ^[40]. Terpenoid examples from fungi show similar activity. For instance, lanostane-type ganoleucoins from *Ganoderma leucocontextum* inhibited HMGCR with $IC_{50} = 8.68$ – $10.2 \mu M$ for the best members, whereas most congeners were weak ($IC_{50} > 100 \mu M$) ^[16]. Additional triterpenes from *Ganoderma* exhibited $IC_{50} = 26.4 \mu M$ (vs. 97.5 μM for a less active analogue), and a marine-derived meroterpenoid showed $IC_{50} = 27.9 \mu M$, both consistent with our series ^[41]. Other non-terpenoid natural inhibitors in similar assays include caffeic acid ($IC_{50} = 10.162 \mu M$) and a cowpea-derived tripeptide QDF ($IC_{50} = 12.8 \mu M$), underlining that low-micromolar activity is common among diverse natural chemotypes ^[42]. By contrast, statins inhibit HMGCR with nanomolar potency in hepatocyte or microsomal systems (lovastatin 4.1 nM, simvastatin 8.0–23 nM, pravastatin 2.0–105 nM in human hepatocytes, and atorvastatin 7.5 nM in rat liver microsomes) emphasizing the expected potency gap while validating that our compound **1** resides near the upper end of natural-product efficacy reported to date ^[43].

4. Conclusion

To sum up, chromatographic methods applied to the ethyl acetate fraction of *P. pavonia* facilitated the identification of six terpenoids. The inhibitory activity of studied tepenoids against HMGCR was evaluated through a comprehensive approach, combining both computational and experimental methodologies. Compounds **1** and **2** successfully docked into the identical binding pocket as the reference drug atorvastatin, indicating their activity as

482 HMGCR inhibitors. The presence of numerous hydrophobic interacting residues suggests a
483 predominantly hydrophobic nature in the binding mode of the isolated terpenes. Conversely,
484 compounds 4 and 6 exhibited a high degree of polar interactions. These results emphasize the
485 diverse modes of interaction between isolated terpenes and HMGCR. The MD simulation
486 results yielded valuable insights into the dynamic behaviors and stabilities of various
487 complexes. Complexes involving isolated terpenes exhibited a notable fluctuation in RMSD
488 profiles, indicative of significant structural variations during the simulation period. The higher
489 RMSD values observed for the tested complexes compared to the free enzyme suggest that
490 these drugs may disrupt the enzyme's stability or induce conformational changes, potentially
491 affecting its function. Particularly, compound **1** displayed the highest fluctuation in drug-to-
492 drug RMSD profiles, suggesting pronounced conformational changes or greater adaptability
493 in its binding conformation with the target enzyme. Moreover, the limited number of hydrogen
494 bonds implies an interaction predominantly driven by hydrophobic or van der Waals forces.
495 Compound **1** also showed the lowest average Rg and SASA values, indicating a highly compact
496 and minimum energy conformation of the compound **1**-HMGCR system and potential
497 stabilization within the enzyme's active site. This suggests stronger binding interactions or a
498 more favorable binding orientation of compound **1** within the HMGCR binding site. In
499 agreement, compound **1** exhibited the most potent HMGCR inhibitory activity assayed *in vitro*.
500 Furthermore, all tested complexes lower average LJ-SR interaction energies compared to their
501 Coul-SR rivals, highlighting the prevailing contribution of van der Waals interactions over
502 electrostatic interactions. This underscores that the binding stability of the complexes is
503 primarily influenced by attractive forces associated with van der Waals interactions rather than
504 Coulombic interactions. The MM/PBSA calculations indicate that compounds **1**, **2**, and **5**

exhibit promising potential as inhibitors of HMG CoA reductase. Their high binding affinities suggest efficacy in modulating the enzyme's activity, showing promise for therapeutic interventions targeting cholesterol biosynthesis pathways.

Conflict of Interest

The authors declare no conflict of interest.

Availability of data and materials

The manuscript and supplementary material contain all data supporting the reported results.

Acknowledgment

Princess Nourah bint Abdulrahman University Researchers Supporting Project Number (PNURSP2025R381), Princess Nourah bint Abdulrahman University, Riyadh, Saudi Arabia.

The authors thank the Centro de Computación Científica of the UAM (CCC-UAM) for the generous allocation of computer time and continued technical support and the support from the project Y2020/EMT-6290 (PRIES-CM) of the Comunidad de Madrid.

Authors' Contributions:

Conceptualization: A.M.M. and E.M.K.; Methodology: A.M.M., E.M.K., R.S.A., S.M.A., and A.L.; Investigation: A.M.M., E.M.K., R.S.A., S.M.A., and A.L.; Data curation: A.M.M., E.M.K., and A.L.; Formal analysis: A.M.M., and E.M.K.; Resources: A.L., S.M.A., and R.S.A.; Supervision: A.M.M. and E.M.K.; Writing-Original draft: A.M.M. and E.M.K.; Writing-review and editing: A.M.M. E.M.K. isolated and characterized the tested terpenoids. All authors read and approved the manuscript.

References

- [1] P. Liao, H. Wang, A. Hemmerlin, D. A. Nagegowda, T. J. Bach, M. Wang, M.-L. Chye, *Plant Cell Reports* **2014**, 33, 1005-1022.
- [2] I. Buhaescu, H. Izzedine, *Clinical Biochemistry* **2007**, 40, 575-584.

- 529 [3] E. F. Oliveira, D. Santos-Martins, A. M. Ribeiro, N. F. Brás, N. S. Cerqueira, S. F.
530 Sousa, M. J. Ramos, P. A. Fernandes, *Expert Opinion on Therapeutic Patents* **2016**, 26,
531 1257-1272.
- 532 [4] Y. Duan, K. Gong, S. Xu, F. Zhang, X. Meng, J. Han, *Signal Transduction and Targeted*
533 *Therapy* **2022**, 7, 265.
- 534 [5] G. Baskaran, S. Salvamani, S. A. Ahmad, N. A. Shaharuddin, P. D. Pattiram, M. Y.
535 Shukor, *Drug Design, Development and Therapy* **2015**, 9, 509-517.
- 536 [6] C. R. Sirtori, *Pharmacological Research* **2014**, 88, 3-11.
- 537 [7] M. O. Germoush, H. A. Elgebaly, S. Hassan, E. M. Kamel, M. Bin-Jumah, A. M.
538 Mahmoud, *Antioxidants* **2020**, 9, 22.
- 539 [8] aR. V. Men'shova, S. P. Ermakova, S. M. Rachidi, A. H. Al-Hajje, T. N. Zvyagintseva,
540 H. M. Kanaan, *Chemistry of Natural Compounds* **2012**, 47, 870-875; bE. M. Abdella,
541 A. M. Mahmoud, A. M. El-Derby, *Pharmaceutical Biology* **2016**, 54, 2496-2504; cA.
542 M. Mahmoud, E. M. Abdella, A. M. El-Derby, E. M. Abdella, *Phytotherapy Research*
543 **2015**, 29, 737-748.
- 544 [9] aI. Jerković, M. Kranjac, Z. Marijanović, M. Roje, S. Jokić, *Molecules* **2019**, 24, 495;
545 bA. J. Mian, E. Percival, *Carbohydrate Research* **1973**, 26, 133-146; cI. Generalić
546 Mekinić, V. Šimat, V. Botić, A. Crnjac, M. Smoljo, B. Soldo, I. Ljubenkov, M. Čagalj,
547 D. Skroza, *Foods* **2021**, 10, 1187; dM. Magdel-Din Hussein, A. Abdel-Aziz, H.
548 Mohamed Salem, *Phytochemistry* **1980**, 19, 2131-2132.
- 549 [10] aN. M. Al-Enazi, A. S. Awaad, M. E. Zain, S. I. Alqasoumi, *Saudi Pharmaceutical*
550 *Journal* **2018**, 26, 44-52; bM. I. Rushdi, I. A. M. Abdel-Rahman, H. Saber, E. Z. Attia,
551 H. A. Madkour, U. R. Abdelmohsen, *South African Journal of Botany* **2021**, 141, 37-
552 48; cM. E. M. Makhlof, M. M. El-Sheekh, A. I. M. El-Sayed, *International Journal of*
553 *Environmental Health Research* **2024**, 34, 1861-1878.
- 554 [11] aE. M. Kamel, N. A. Ahmed, A. A. El-Bassuony, O. E. Hussein, B. Alrashdi, S. A.
555 Ahmed, A. M. Lamsabhi, H. H. Arab, A. M. Mahmoud, *Combinatorial Chemistry &*
556 *High Throughput Screening* **2022**, 25, 1336-1344; bE. M. Kamel, A. Bin-Ammar, A.
557 A. El-Bassuony, M. M. Alanazi, A. Altharawi, A. F. Ahmeda, A. S. Alanazi, A. M.
558 Lamsabhi, A. M. Mahmoud, *RSC Advances* **2023**, 13, 12361-12374; cB. Tan, W. Lan,

- 559 S. Zhang, H. Deng, Y. Qiang, A. Fu, Y. Ran, J. Xiong, R. Marzouki, W. Li, *Colloids*
560 *and Surfaces A: Physicochemical and Engineering Aspects* **2022**, 645, 128892.
- 561 [12] aE. M. Kamel, A. M. Tawfeek, A. A. El-Bassuony, A. M. Lamsabhi, *Organic &*
562 *Biomolecular Chemistry* **2023**; bE. M. Kamel, A. M. Tawfeek, A. A. El-Bassuony, A.
563 M. Lamsabhi, *New Journal of Chemistry* **2023**.
- 564 [13] aE. M. Kamel, A. M. Lamsabhi, *Organic & Biomolecular Chemistry* **2021**, 19, 9031-
565 9042; bA. Sajid, N. Mehr un, A. Sajid, E. Ahmed, K. Umm i, A. Sharif, Q. Manzoor,
566 S. H. Al-Mijalli, M. Iqbal, *Journal of Molecular Structure* **2024**, 1312, 138549; cA.
567 Sajid, Q. Manzoor, A. Sajid, N. Mehr un, F. Imtiaz, M. A. Mumtaz, N. Fatima, O. A.
568 Mohammed, M. A. Abdel-Reheim, M. Iqbal, *Journal of Molecular Structure* **2025**,
569 1321, 139675.
- 570 [14] E. M. Kamel, A. M. Lamsabhi, *Organic & Biomolecular Chemistry* **2020**, 18, 3334-
571 3345.
- 572 [15] aM. Kaffash, S. Tolou-Shikhzadeh-Yazdi, S. Soleimani, S. Hoseinpoor, M. R. Saberi,
573 J. Chamani, *Spectrochimica Acta Part A: Molecular and Biomolecular Spectroscopy*
574 **2024**, 309, 123815; bR. S. Alruhaimi, A. M. Mahmoud, I. Elbagory, A. F. Ahmeda, A.
575 A. El-Bassuony, A. M. Lamsabhi, E. M. Kamel, *Bioorganic Chemistry* **2024**, 147,
576 107397; cJ. Chamani, *Journal of Molecular Structure* **2010**, 979, 227-234.
- 577 [16] J. Zhang, K. Ma, J. Han, K. Wang, H. Chen, L. Bao, L. Liu, W. Xiong, Y. Zhang, Y.
578 Huang, H. Liu, *Fitoterapia* **2018**, 130, 79-88.
- 579 [17] O. Trott, A. J. Olson, *Journal of Computational Chemistry* **2010**, 31, 455-461.
- 580 [18] M. J. Frisch, G. W. Trucks, H. B. Schlegel, G. E. Scuseria, M. A. Robb, J. R.
581 Cheeseman, G. Scalmani, V. Barone, G. A. Petersson, H. Nakatsuji, X. Li, M. Caricato,
582 A. V. Marenich, J. Bloino, B. G. Janesko, R. Gomperts, B. Mennucci, H. P. Hratchian,
583 J. V. Ortiz, A. F. Izmaylov, J. L. Sonnenberg, Williams, F. Ding, F. Lipparini, F. Egidi,
584 J. Goings, B. Peng, A. Petrone, T. Henderson, D. Ranasinghe, V. G. Zakrzewski, J. Gao,
585 N. Rega, G. Zheng, W. Liang, M. Hada, M. Ehara, K. Toyota, R. Fukuda, J. Hasegawa,
586 M. Ishida, T. Nakajima, Y. Honda, O. Kitao, H. Nakai, T. Vreven, K. Throssell, J. A.
587 Montgomery Jr., J. E. Peralta, F. Ogliaro, M. J. Bearpark, J. J. Heyd, E. N. Brothers, K.
588 N. Kudin, V. N. Staroverov, T. A. Keith, R. Kobayashi, J. Normand, K. Raghavachari,
589 A. P. Rendell, J. C. Burant, S. S. Iyengar, J. Tomasi, M. Cossi, J. M. Millam, M. Klene,

590 C. Adamo, R. Cammi, J. W. Ochterski, R. L. Martin, K. Morokuma, O. Farkas, J. B.
591 Foresman, D. J. Fox, Wallingford, CT, **2016**.

592 [19] aC. Lee, W. Yang, R. G. Parr, *Physical review B* **1988**, 37, 785; bA. D. Becke, *Physical*
593 *review A* **1988**, 38, 3098.

594 [20] W. J. Hehre, L. Radom, P. v. R. Schleyer, J. A. Pople, *Ab initio molecular orbital theory*,
595 *Vol. 67*, Wiley New York et al., **1986**.

596 [21] S. Grimme, A. Hansen, J. G. Brandenburg, C. Bannwarth, *Chemical Reviews* **2016**,
597 *116*, 5105-5154.

598 [22] aY.-X. Yu, *The Journal of Physical Chemistry C* **2019**, 123, 205-213; bY.-X. Yu,
599 *Applied Surface Science* **2021**, 546, 149062.

600 [23] aP. Bauer, B. Hess, E. Lindahl, *November* **2022**, 16, 2022; bM. J. Abraham, T. Murtola,
601 R. Schulz, S. Páll, J. C. Smith, B. Hess, E. Lindahl, *SoftwareX* **2015**, 1-2, 19-25.

602 [24] J. Huang, S. Rauscher, G. Nawrocki, T. Ran, M. Feig, B. L. de Groot, H. Grubmüller,
603 A. D. MacKerell, Jr., *Nat Methods* **2017**, 14, 71-73.

604 [25] A. D. MacKerell, Jr., D. Bashford, M. Bellott, R. L. Dunbrack, Jr., J. D. Evanseck, M.
605 J. Field, S. Fischer, J. Gao, H. Guo, S. Ha, D. Joseph-McCarthy, L. Kuchnir, K.
606 Kuczera, F. T. K. Lau, C. Mattos, S. Michnick, T. Ngo, D. T. Nguyen, B. Prodhom, W.
607 E. Reiher, B. Roux, M. Schlenkrich, J. C. Smith, R. Stote, J. Straub, M. Watanabe, J.
608 Wiórkiewicz-Kuczera, D. Yin, M. Karplus, *The Journal of Physical Chemistry B* **1998**,
609 *102*, 3586-3616.

610 [26] B. Hess, C. Kutzner, D. Van Der Spoel, E. Lindahl, *Journal of chemical theory and*
611 *computation* **2008**, 4, 435-447.

612 [27] M. Parrinello, A. Rahman, *Journal of Applied physics* **1981**, 52, 7182-7190.

613 [28] aB. R. Miller, III, T. D. McGee, Jr., J. M. Swails, N. Homeyer, H. Gohlke, A. E.
614 Roitberg, *Journal of Chemical Theory and Computation* **2012**, 8, 3314-3321; bS.
615 Genheden, U. Ryde, *Expert Opinion on Drug Discovery* **2015**, 10, 449-461.

616 [29] M. S. Valdés-Tresanco, M. E. Valdés-Tresanco, P. A. Valiente, E. Moreno, *Journal of*
617 *Chemical Theory and Computation* **2021**, 17, 6281-6291.

618 [30] K. Wang, L. Bao, W. Xiong, K. Ma, J. Han, W. Wang, W. Yin, H. Liu, *J Nat Prod* **2015**,
619 *78*, 1977-1989.

- 620 [31] aH. Duan, Y. Takaishi, H. Momota, Y. Ohmoto, T. Taki, *Phytochemistry* **2002**, 59, 85-
621 90; bS. U. Choi, M. C. Yang, K. H. Lee, K. H. Kim, K. R. Lee, *Archives of pharmacal*
622 *research* **2007**, 30, 1067-1074.
- 623 [32] H. C. Kwon, K. R. Lee, *Archives of pharmacal research* **2001**, 24, 194-197.
- 624 [33] aZ. He, A. Zhang, L. Ding, X. Lei, J. Sun, L. Zhang, *Fitoterapia* **2010**, 81, 1125-1128;
625 bR. Tanaka, S. Matsunaga, *Phytochemistry* **1989**, 28, 1699-1702.
- 626 [34] aJ.-H. Park, D.-G. Lee, S.-W. Yeon, H.-S. Kwon, J.-H. Ko, D.-J. Shin, H.-S. Park, Y.-
627 S. Kim, M.-H. Bang, N.-I. Baek, *Archives of pharmacal research* **2011**, 34, 533-542;
628 bA. J. Aasen, B. Kimland, C. Enzell, *Acta chemica scandinavica* **1973**.
- 629 [35] aX. Liu, Q. X. Wu, Y. P. Shi, *Journal of the Chinese Chemical Society* **2005**, 52, 369-
630 374; bA. Yurchenko, O. Smetanina, A. Kalinovskii, N. Kirichuk, E. Yurchenko, S. S.
631 Afiyatullo, *Chemistry of Natural Compounds* **2013**, 48, 996-998.
- 632 [36] aM. Häusler, A. Montag, *Zeitschrift für Lebensmittel-Untersuchung und Forschung*
633 **1989**, 189, 113-115; bH. Fukui, K. Koshimizu, S. Usuda, Y. Yamazaki, *Agricultural*
634 *and Biological Chemistry* **1977**, 41, 175-180.
- 635 [37] Y. Yu, S. Fujimoto, *Science China Chemistry* **2013**, 56, 524-532.
- 636 [38] M. Y. Lobanov, N. S. Bogatyreva, O. V. Galzitskaya, *Molecular Biology* **2008**, 42, 623-
637 628.
- 638 [39] aM. Rivera, M. Dommett, R. Crespo-Otero, *Journal of Chemical Theory and*
639 *Computation* **2019**, 15, 2504-2516; bM. J. Van Vleet, A. J. Misquitta, A. J. Stone, J. R.
640 Schmidt, *Journal of Chemical Theory and Computation* **2016**, 12, 3851-3870.
- 641 [40] S. H. Lin, K. J. Huang, C. F. Weng, D. Shiuan, *Drug Des Devel Ther* **2015**, 9, 3313-
642 3324.
- 643 [41] aK. Wang, L. Bao, W. Xiong, K. Ma, J. Han, W. Wang, W. Yin, H. Liu, *Journal of*
644 *Natural Products* **2015**, 78, 1977-1989; bJ. Zhang, K. Ma, H. Chen, K. Wang, W.
645 Xiong, L. Bao, H. Liu, *The Journal of Antibiotics* **2017**, 70, 915-917.
- 646 [42] M. Silva, B. Philadelpho, J. Santos, V. Souza, C. Souza, V. Santiago, J. Silva, C. Souza,
647 F. Azeredo, M. Castilho, E. Cilli, E. Ferreira, *International Journal of Molecular*
648 *Sciences* **2021**, 22, 11067.
- 649 [43] aJ. R. Burnett, L. J. Wilcox, D. E. Telford, S. J. Kleinstiver, P. H. R. Barrett, R. S.
650 Newton, M. W. Huff, *Arteriosclerosis, Thrombosis, and Vascular Biology* **1997**, 17,

651 2589-2600; bL. H. Cohen, R. E. van Leeuwen, G. C. van Thiel, J. F. van Pelt, S. H.
652 Yap, *Biopharm Drug Dispos* **2000**, 21, 353-364; cA. K. van Vliet, G. C. F. van Thiel,
653 R. H. Huisman, H. Moshage, S. H. Yap, L. H. Cohen, *Biochimica et Biophysica Acta*
654 (*BBA*) - *Lipids and Lipid Metabolism* **1995**, 1254, 105-111.

655

656

657 Tables:

658 Table 1. Results of molecular docking of the tested compounds against HMGCR.

	Lowest binding energy (kcal/mol)	Polar interacting residues	Hydrophobic interacting residues
1	-5.7	Tyr517	Tyr519, Val522, Cys527, Val530, Gly532, Tyr533, Leu811, and Gln814
2	-6.0	Met534	Tyr519, Val522, Cys527, Gly532, Tyr533, Leu811, and Gln814
3	-5.6	Asp653	Phe628, Gly652, Ala654, Met659, Val805, and Ala826
4	-5.6	Ser651, Asp653, and Ala654	Ser626, Arg627, Gly652, Met659, Val805, and Ala826
5	-5.9	Ser651	Phe628, Gly652, Asp653, Ala654, Met659, Val805, Gly806, and Ala826
6	-5.5	Asn686, Thr689, and Ala695	Tyr644, Tyr687, Ala694, and Ile696
Atorvastatin	-6.5	Met534, Gly765, and Gly808	Tyr517, Cys526, Cys527, Ile531, Gly532, Tyr533, Ile536, Ile762, Gln766, Leu811, and Gln814

659

660 Table 2. Average Coul-SR and LJ-SR interaction energies of tested compounds-HMGCR
 661 complexes.

	Coul-SR interaction energy		LJ-SR interaction energy	
	Average (kJ/mol)	RMSD (nm)	Average (kJ/mol)	RMSD (nm)
1	-9.77 ± 4.3	14.59	-40.51 ± 15	32.89
2	-15.96 ± 2.9	16.76	-69.03 ± 2.8	13.49
3	-3.95 ± 2.0	9.21	-17.55 ± 11	25.07
4	-29.08 ± 2.3	17.30	-84.38 ± 4.0	14.07
5	-50.89 ± 2.2	12.80	-76.30 ± 2.9	12.53
6	-1.93 ± 3.1	10.69	-83.78 ± 3.3	14.37

662

663

664 Table 3. The results of MM/PBSA calculations (kJ/mol).

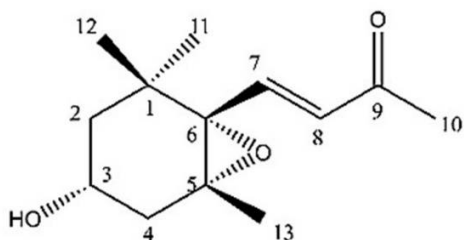
System	ΔE_{vdw}	ΔE_{ele}	ΔG_{solv}	ΔG_{gas}	ΔG_{total}
Compound 1	-7.13 ± 0.83	-4.12 ± 0.56	4.25 ± 0.31	-11.25 ± 1.2	-7.0 ± 1.0
Compound 2	-6.55 ± 0.32	-4.11 ± 0.14	3.69 ± 0.16	-10.66 ± 0.36	-6.97 ± 0.38
Compound 3	-2.12 ± 0.11	-0.35 ± 0.16	1.27 ± 0.22	-2.47 ± 0.19	-1.20 ± 0.29
Compound 4	-1.18 ± 0.36	-0.39 ± 0.40	1.89 ± 0.11	-1.57 ± 0.54	0.32 ± 0.55
Compound 5	-6.84 ± 0.62	-3.41 ± 1.11	3.19 ± 1.84	-10.25 ± 1.27	-7.06 ± 2.24
Compound 6	-6.71 ± 0.94	-2.17 ± 0.59	3.46 ± 0.31	-8.88 ± 1.53	-5.42 ± 1.14

665

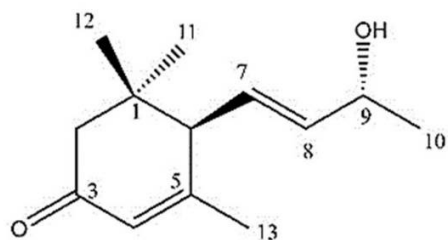
666

667

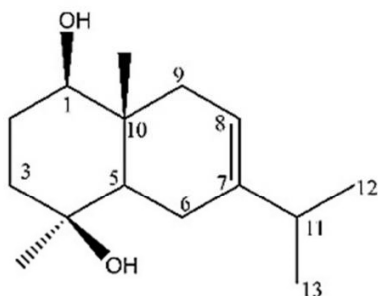
668 Figures:



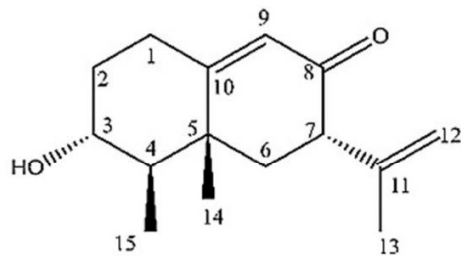
Compound 1



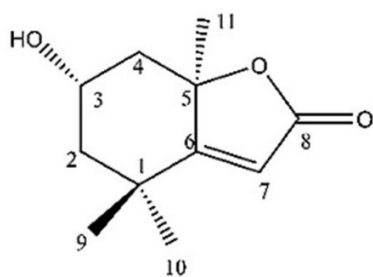
Compound 4



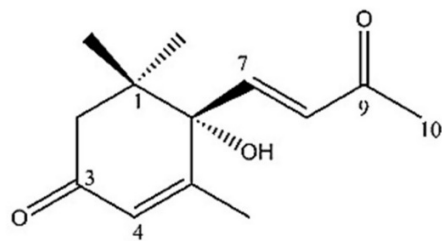
Compound 2



Compound 5



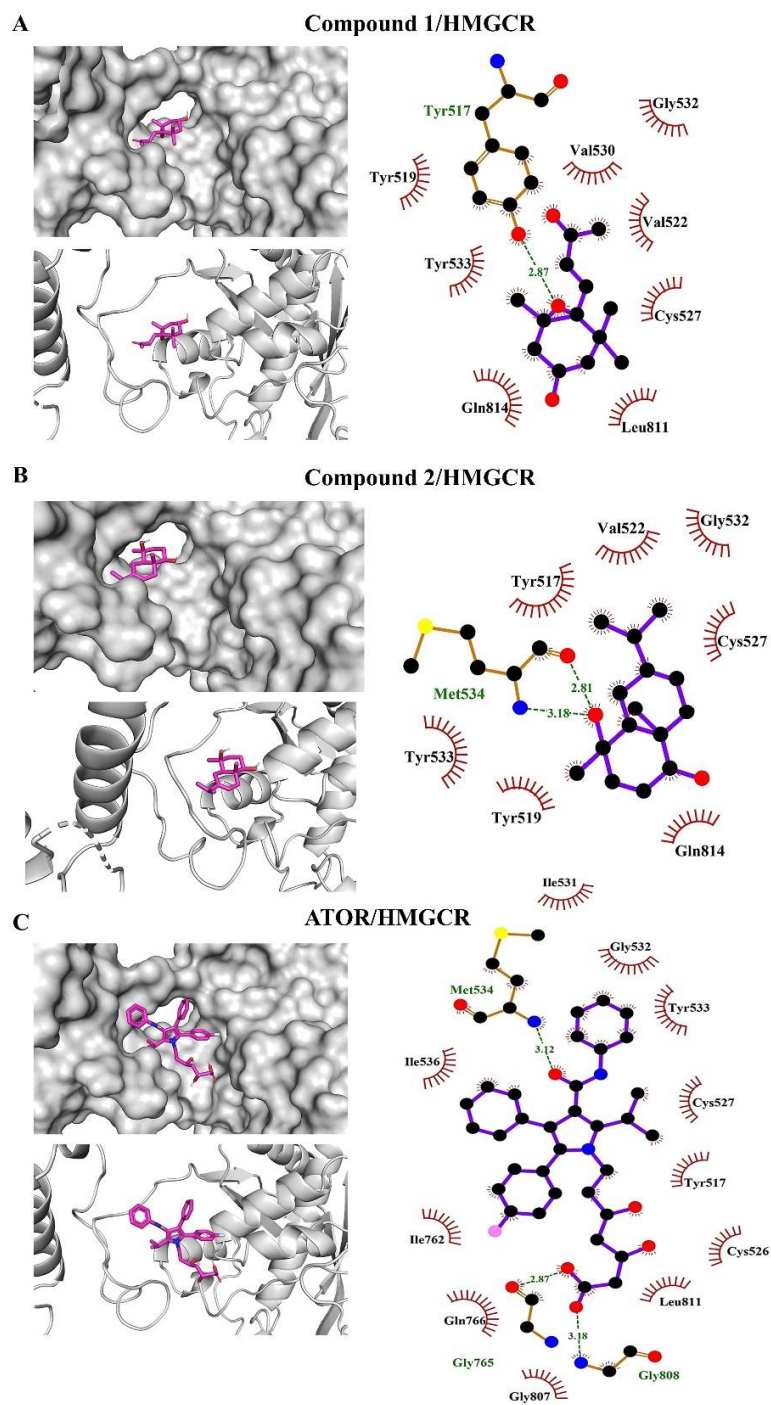
Compound 3



Compound 6

669

670 Figure 1. Structures of EAFCS-isolated compounds.

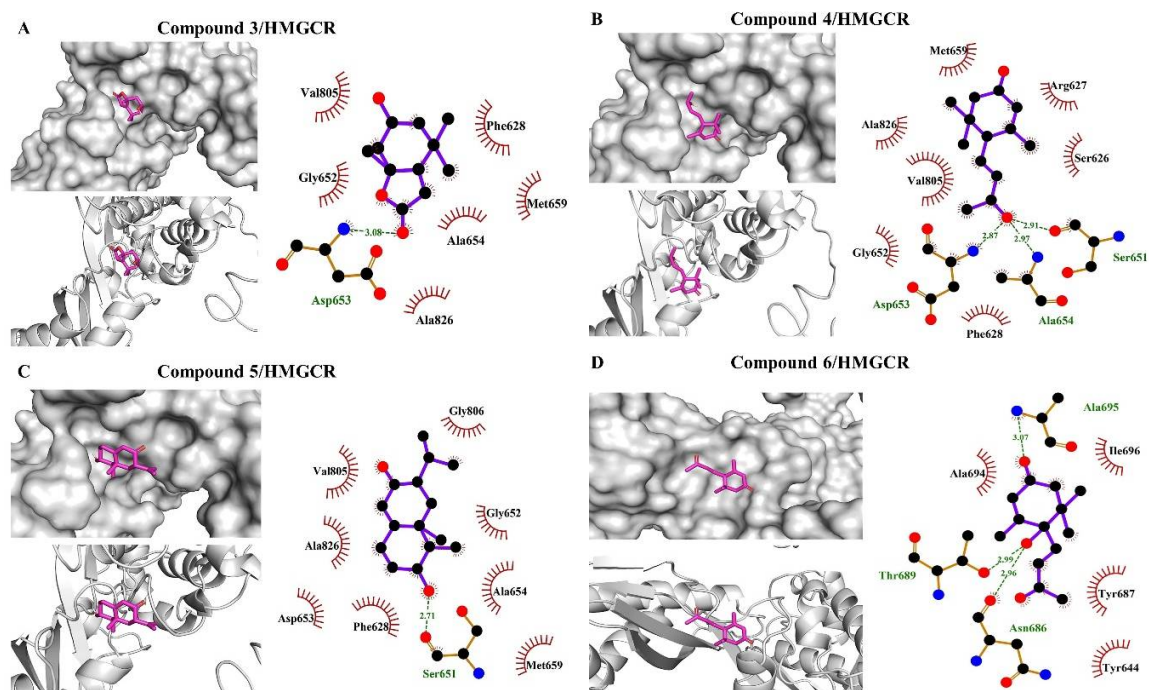


671

672 Figure 2. Binding site interactions of compound 1 (A), compound 2 (B), and atorvastatin (C)

673 with HMGCR. Black, red, blue and yellow circles refer to carbon, oxygen, nitrogen, and sulfur

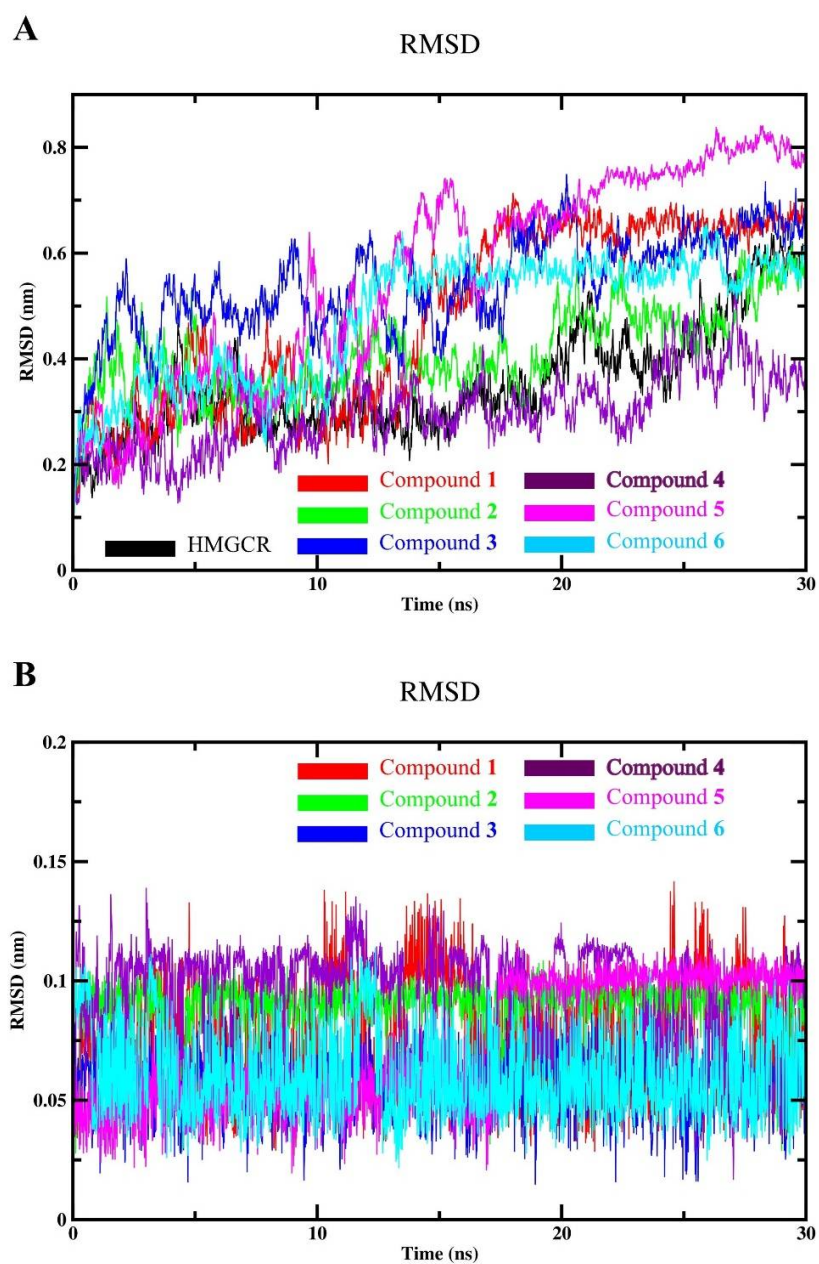
674 atoms, respectively.



675

676 Figure 3. Binding site interactions of compounds **3** (A), **4** (B), **5** (C), and **6** (D) with HMGR.

677 Black, red, and blue circles refer to carbon, oxygen, and nitrogen atoms, respectively.

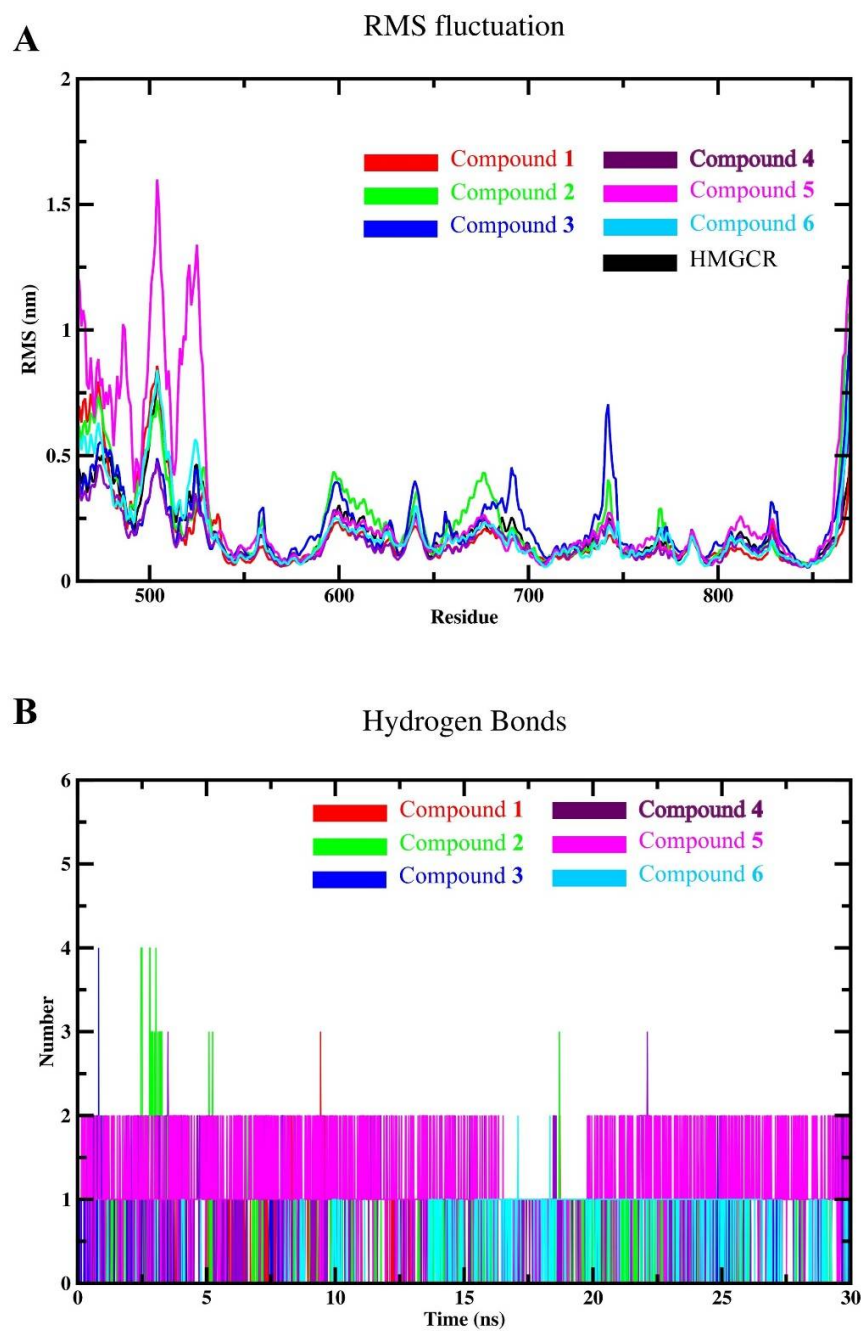


678

679 Figure 4. MD simulation analysis of HMGCR and its complexes with *P. pavonia* compounds;

680 (A) Backbone RMSD of the unbound enzyme and compound-enzyme complexes and (B)

681 RMSD of isolated compounds (300 K).

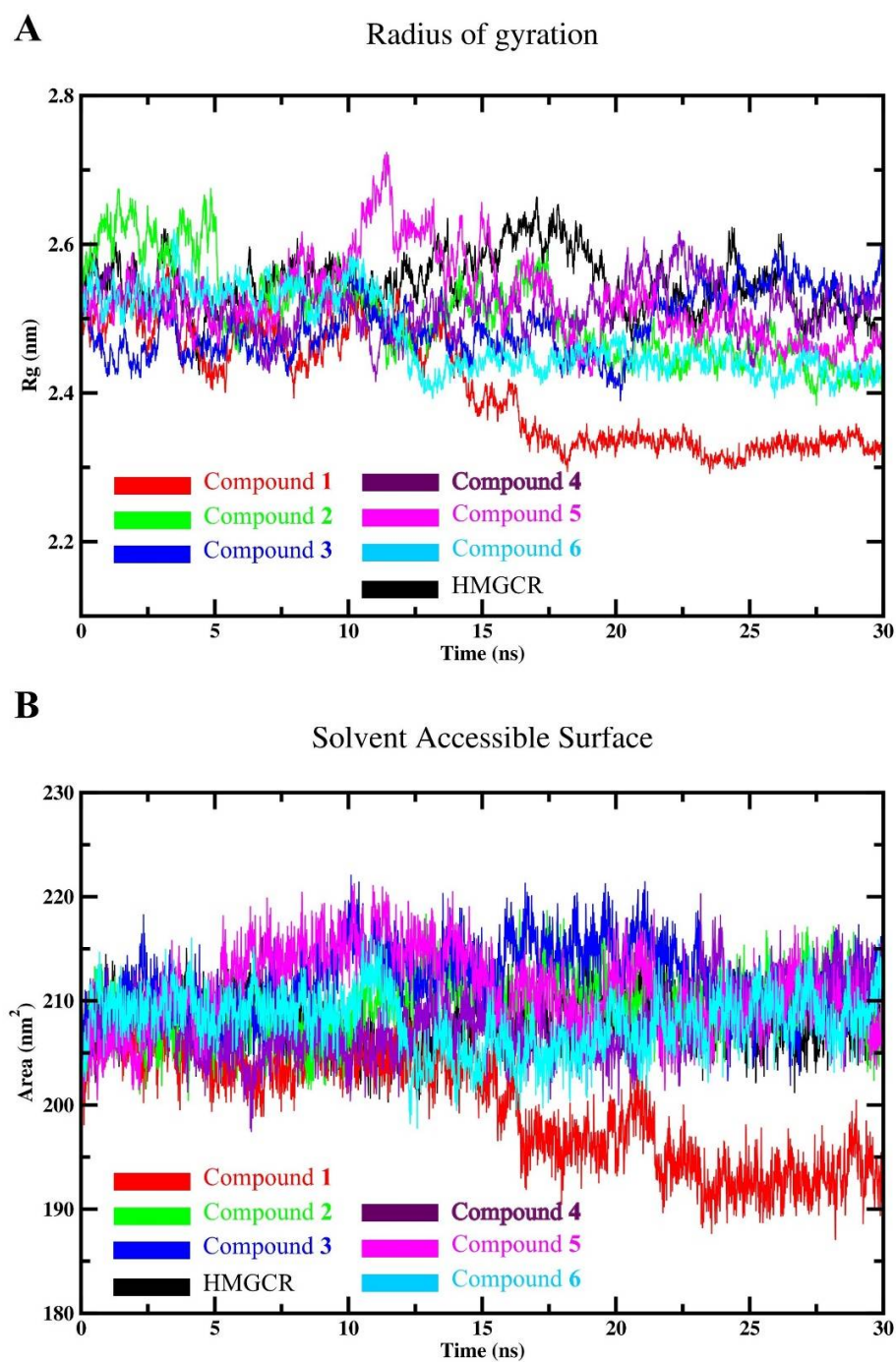


682

683 Figure 5. MD simulation analysis of HMGCR and its complexes with *P. pavonia* compounds;

684 (A) Backbone RMSF per residue number for the enzyme and compound-enzyme complexes

685 and (B) Hydrogen bonding profile of the compound-enzyme complexes (300 K).

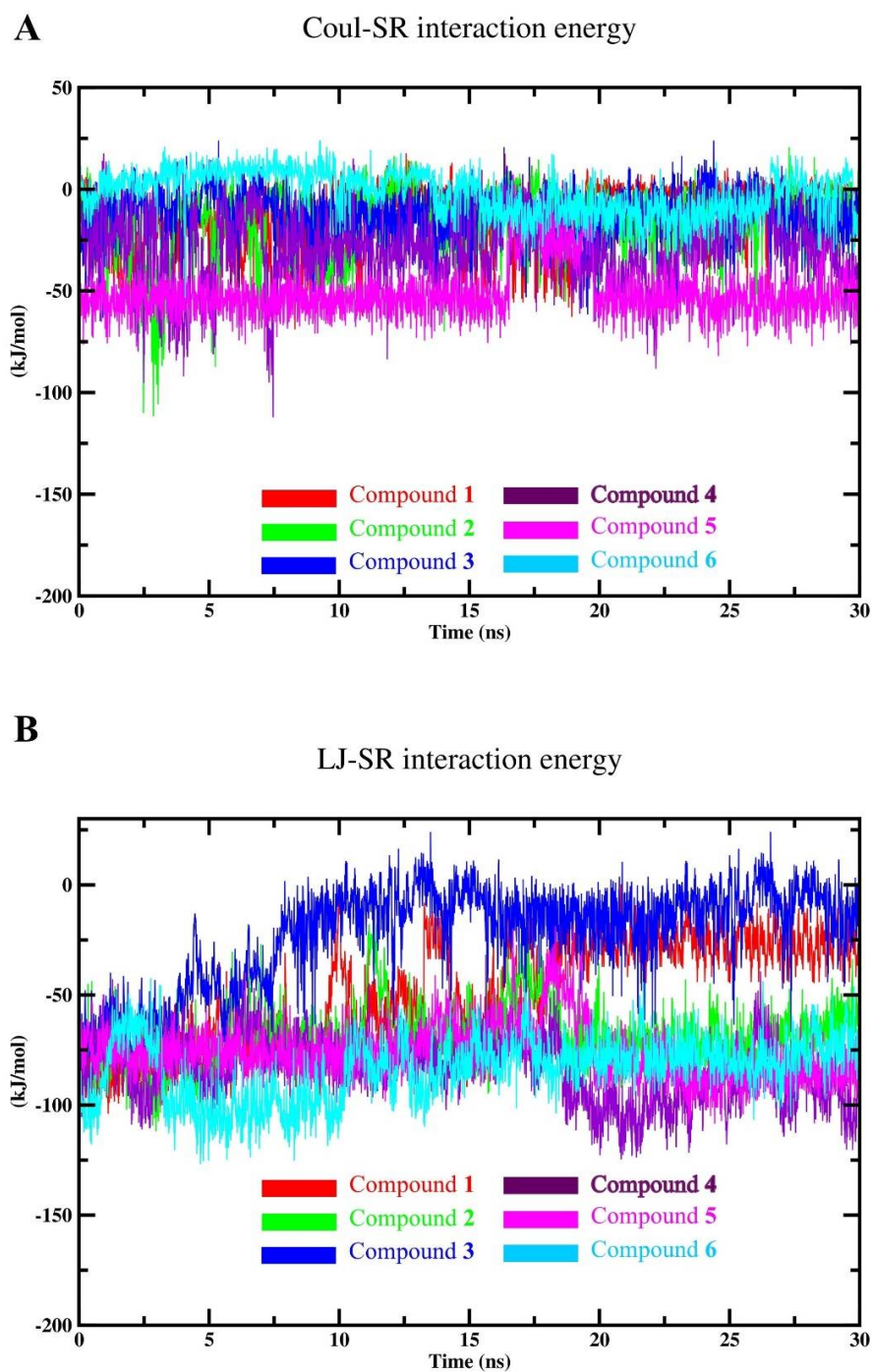


686

687 Figure 6. MD simulation analysis of HMGCR and its complexes with *P. pavonia* compounds;

688 (A) Protein radius of gyration for the enzyme and compound-enzyme complexes and (B)

689 Protein SASA of the enzyme and various complexes (300 K).

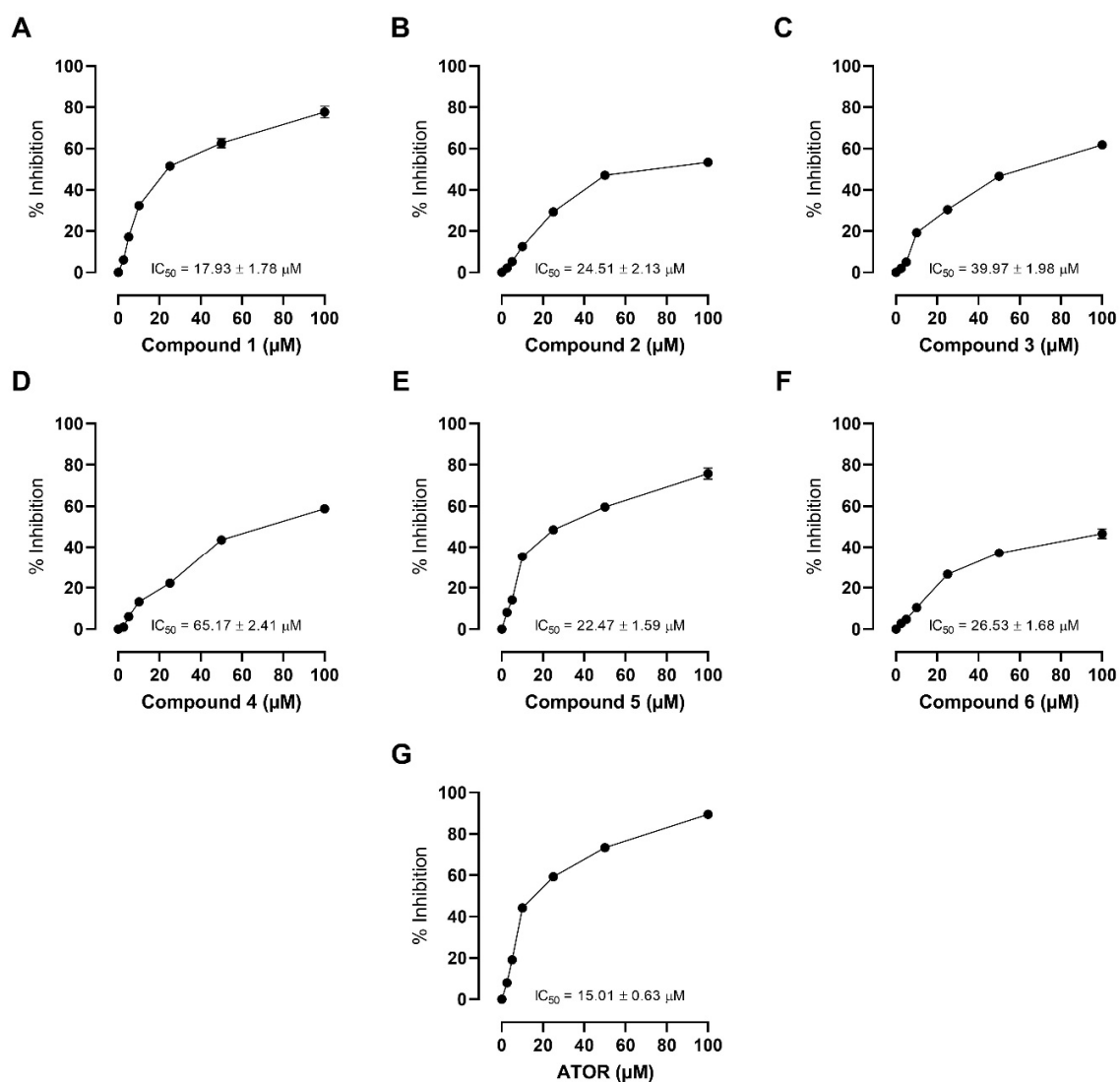


690

691 Figure 7. MD simulation analysis of HMGCR and its complexes with *P. pavonia* compounds;

692 (A) Coulomb-SR interactions energies and (B) Lennard-Jones-SR interactions energies of the

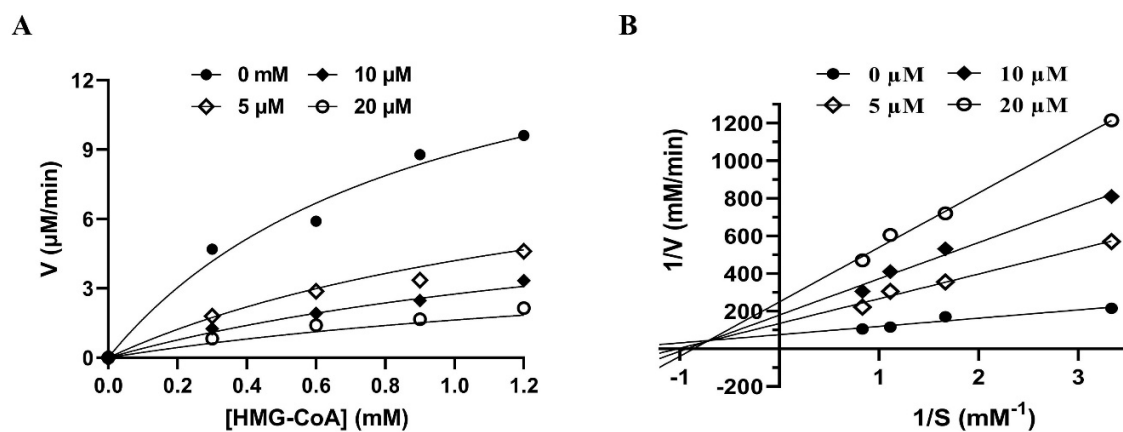
693 enzyme amino acid residues with isolated compounds (300 K).



694

695 Figure 8. HMGCR inhibitory activity *P. pavonia* compounds (A-F) and atorvastatin (G). Data

696 are mean \pm SD, N = 3.



697

698 Figure 9. Michaelis–Menten (A) and Lineweaver–Burk (B) plots of HMGCR inhibitory

699 activity of compound **1**. Data are mean \pm SD, $N = 3$.